ELSEVIER

Journal of Hazardous Materials 41 (1995) 3–30

JOURNAL OF HAZARDOUS MATERIALS

Formation of hydroxyl radicals, hydrogen peroxide and aqueous electrons by pulsed streamer corona discharge in aqueous solution

A.A. Joshi, B.R. Locke*, P. Arce*, W.C. Finney

Department of Chemical Engineering, FAMU/FSU College of Engineering, Tallahassee, FL 32316-2175, USA

Received 1 March 1994; accepted in revised form 6 September 1994

Abstract

The initiation reaction rate constants for the formation of hydroxyl radicals, hydrogen peroxide, and aqueous electrons using a pulsed streamer corona discharge in aqueous solutions are determined in the present study. The free radical scavenging property of carbonate ions was used to determine the initiation rate constants for the formation of hydroxyl radicals and hydrogen peroxide from the pulsed streamer corona discharge. The effects of average current, voltage, and power input on the initiation rate constants were also studied. A reactor model including known chemical reaction kinetics was developed for the degradation of phenol, and the initiation rate constant for aqueous electrons was determined by fitting the experimental data of phenol degradation to the model. Transient concentration profiles predicted by the model were compared to those of experiments for the formation of hydrogen peroxide in deionized water and for the degradation of hydroquinone. It was observed that the model results match experimental results satisfactorily for the formation of hydrogen peroxide and qualitatively follow the experimental results for the degradation of hydroquinone. The model was improved by considering that the reaction rate constants vary with the current in the reactor. The current was observed to vary with time for the cases where no salts were added to the reactor. It was observed that the improved model follows the experimental results satisfactorily for high initial concentrations ($> 5.4 \times 10^{-5} M$) of hydroquinone.

1. Introduction

A number of alternative processes such as UV photolysis [1,2], direct ozonation [3,4], photo-catalysis [5], and electron beam treatment [6,7], have been applied to degrade organic pollutants in aqueous solutions. Recently, a new process utilizing a pulsed streamer corona discharge has been demonstrated to be effective at removing phenol, benzene, and other small aromatic compounds in aqueous solutions on

*Corresponding authors.

SSDI 0304-3894(94)00099-9

a laboratory scale [8,9]. A corona discharge is an ionic and electronic emission from a high voltage corona, characterized by the formation and flow of positive ions, negative ions, and electrons in an electric field between two or more electrodes. Specifically, the pulsed streamer corona technique used in the present investigation uses a high voltage electric discharge (25–40 kV) having a very short pulse width (approximately 500–1000 ns). These unique specifications produce a corona that differs markedly from normal continuous discharge (dc corona), ac discharge, and long-pulse (μs–ms) corona discharge. One very important consequence of the brief duration of the pulse is that it minimizes the power normally wasted on ionic migration because the mobility of ions is much less than that of electrons [10]. Ions do not contribute to free radical formation, however energetic electrons do actively promote these reactions. In the present investigation streamer corona is produced by a rotating spark gap pulsed power supply, capable of supplying the reactor discharge electrode with, in this case, high voltage (25–40 kV), short duration (200–2000 ns), fast rise time (20–100 ns), repetitive (60 Hz), electrical pulses.

The pulsed corona discharge gives rise to the formation of hydroxyl radicals, hydrogen peroxide, and aqueous electrons, as well as several other species [10–12]. The major reactive species involved in the degradation of organic contaminants are hydroxyl radicals and hydrogen peroxide [8]. Hydroxyl radicals directly attack organic compounds leading to the oxidation of these compounds. Hydrogen peroxide is important in organic contaminant degradation because in the presence of iron it produces large numbers of hydroxyl radicals through Fenton's reaction [13]. The presence of free radical scavengers such as phosphate or carbonate ions in the solution reduces the rate of breakdown of the organic compound [3, 11], as in any advanced method that utilizes hydroxyl radicals. In addition to these scavenging effects, high salt concentration will increase the conductivity of the solution, which will in turn lead to decreased streamer formation and lower quantities of reactive radicals [10]. In general, these factors can be controlled and the system can be operated to minimize their effects; however, they can also be utilized, as shown in the present work, to determine reaction rate constants.

The pulsed streamer corona technique described above involves a very complex set of chemical reactions where several parameters such as pulsed voltage level, solution composition, pH, and conductivity play critical roles. It is, therefore, essential to develop a basic understanding of the chemical reaction kinetics involved in the pulsed streamer corona discharge process in order to design, scale-up, and operate a pulsed streamer corona reactor on a larger scale and to assess its usefulness for degrading other hazardous wastes. It is also necessary to estimate the power efficiency of this process for future comparisons between this method and other competing processes such as electron beam treatment, γ-radiation treatment, UV photolysis, direct injection of ozone and/or hydrogen peroxide, and other electric field-generating hydrogen peroxide methods [14]. The specific goals of the present research are: (1) to determine the rates of formation of radical and molecular species, specifically hydroxyl radicals, hydrogen peroxide, and aqueous electrons involved in the pulsed streamer corona process in the aqueous phase, (2) to develop a reactor model for describing the pulsed streamer corona discharge process in the aqueous phase, and (3) to study the effect of

voltage input on the rates of formation of radical and molecular species for a given range of input values.

In the present study, a series of experiments was performed with different levels of carbonate concentration to determine the yield of hydroxyl radicals and hydrogen peroxide. The reactor model consists of the molar species balance equations for each chemical species involved in the process under the assumptions of a well-mixed reactor solution and isothermal conditions. The kinetics of the process is described by a set of reactions where the pseudo-steady state assumption was made for all radical and ionic species. As a result of these assumptions, the reactor model consists of a system of algebraic equations and ordinary differential equations with initial values. The rate of formation of aqueous electrons was determined by fitting the experimental data for phenol degradation to the model. The effects of the applied pulsed voltage on the initiation rate constants were studied. The model was then tested for hydroquinone degradation for different initial concentrations of hydroquinone, and for the formation of hydrogen peroxide in deionized water.

2. Chemical reactions

The pulsed streamer corona discharge in the aqueous phase gives rise to the formation of several species [10]. Since the process involves excitation, ionization, and dissociation of water, the reaction mechanism may be similar to those in radiolytic processes such as γ-radiation, electron beam radiation, pulsed radiolysis and photochemical processes which produce radical and molecular species through excitation and ionization of the treated material [15–17]. In addition, the pulsed streamer corona process produces charged particles having energies of about 5–20 eV. Therefore, the reactions occurring in the aqueous phase are assumed to be as follows [18–23]:

$$H_2O \xrightarrow{k_{OH}} H^{\cdot} + OH^{\cdot}, \tag{1}$$

$$H_2O \xrightarrow{k_{H_2O_2}} \tfrac{1}{2}H_2O_2 + \tfrac{1}{2}H_2, \tag{2}$$

$$H_2O \xrightarrow{k_{e_{aq}^-}} H_2O^+ + e_{aq}^-. \tag{3}$$

Reactions (1–3) are assumed to be initiated by the pulsed streamer corona and will therefore be directly affected by the characteristics of the discharge. These reactions are common to radiation and photochemical processes [13, 22]. Since the water concentration remains approximately constant, these reactions were assumed to be zero-order. When there is an organic compound such as phenol present in the system, the hydroxyl radicals react with the organic compound to produce oxidation products. It has been found that the rate of degradation of phenol in a reactor vessel having a point-to-plane electrode geometry depends upon the applied electric field [11]. This

suggests that the formation of radical and molecular species occurring in the process depends upon the energy input. Therefore, these three rate constants were assumed to be functions of energy input. Since the mechanism involves excitation, dissociation and ionization, larger energy input should enhance these processes and will produce more of these species. It is thus necessary to determine quantitatively the additional amount of reactive species produced by the increased energy input.

In order to properly describe the chemical processes involved in the corona discharge reactor, propagation and termination reactions must also be assumed to occur. The propagation reactions are given by

$$H^{\cdot} + O_2 \xrightarrow{k_4} HO_2^{\cdot}, \tag{4}$$

$$H^{\cdot} + H_2O_2 \xrightarrow{k_5} H_2O + OH^{\cdot}, \tag{5}$$

$$OH^{\cdot} + H_2O_2 \xrightarrow{k_6} H_2O + HO_2^{\cdot}, \tag{6}$$

$$H_2O^{+} + H_2O \xrightarrow{k_7} OH^{\cdot} + H_3O^{+}, \tag{7}$$

$$e_{aq}^{-} + OH^{\cdot} \xrightarrow{k_8} OH^{-}, \tag{8}$$

$$e_{aq}^{-} + H^{\cdot} + H_2O \xrightarrow{k_9} OH^{-} + H_2, \tag{9}$$

$$e_{aq}^{-} + H_2O_2 \xrightarrow{k_{10}} OH^{\cdot} + OH^{-}, \tag{10}$$

$$e_{aq}^{-} + H_2O \xrightarrow{k_{11}} H^{\cdot} + OH^{-} \tag{11}$$

and the termination reactions are given by

$$H^{\cdot} + OH^{\cdot} \xrightarrow{k_{12}} H_2O, \tag{12}$$

$$2OH^{\cdot} \xrightarrow{k_{13}} H_2O_2, \tag{13}$$

$$2HO_2^{\cdot} \xrightarrow{k_{14}} H_2O_2 + O_2, \tag{14}$$

$$H^{\cdot} + HO_2^{\cdot} \xrightarrow{k_{15}} H_2O_2, \tag{15}$$

$$2H^{\cdot} \xrightarrow{k_{16}} H_2, \tag{16}$$

$$HO_2^{\cdot} + OH^{\cdot} \xrightarrow{k_{17}} H_2O + O_2, \tag{17}$$

$$H_3O^+ + OH^- \xrightarrow{k_{18}} 2H_2O, \tag{18}$$

$$H_2O^+ + e_{aq}^- \xrightarrow{k_{19}} H_2O. \tag{19}$$

Reactions (4)–(19) are common to most oxidation processes such as UV photolysis, γ-radiation process, and electron beam treatment [13, 22]. It is clear from these reactions that the radical and molecular species formed by Eqs. (1)–(3) in the pulsed streamer corona discharge participate in a number of subsequent reactions. In the present study it is assumed that the rates of reactions (4)–(19) do not depend directly on the corona discharge. One of the goals of the present study is to determine the zero-order rate constants of reactions (1)–(3) for this particular system in order to develop a basic knowledge about the system that will allow for a quantitative comparison with other treatment processes.

The hydroxyl radicals formed from pulsed streamer corona react with phenol to produce oxidation products. These oxidation products again react with hydroxyl radicals. The reaction mechanism for the oxidation of phenol via hydroxyl radical attack is shown in Table 1. It has been reported that the primary oxidation products of phenol due to hydroxyl radical attack are hydroquinone (1,4-dihydroxybenzene), catechol (1,2-dihydroxybenzene), and resorcinol (1,3-dihydroxybenzene) [24–26]. The secondary products are pyrogallol (1,2,3-trihydroxybenzene), 1,2,4-trihydroxybenzene, p-quinone (1,4-benzoquinone), 2-hydroxy-1,4-benzoquinone [24–26]. Table 1 also shows some of the reactions involved in the oxidation of hydroquinone. The reactions shown in this table are assumed to be irreversible and there is no strict balance on hydrogen since these are not elementary reactions and the eventual products are assumed to be water and CO_2.

3. Modeling of the pulsed streamer corona reactor

A reactor model including the chemical reactions discussed above was developed to describe the behavior of the corona discharge process. In the model development it is assumed that: (1) the reactor is isothermal and well-mixed, (2) the volume of the reactor is approximately constant, (3) the pseudo-steady state approximation is used for all radical species since the radical species are not stable, and the same assumption was made for all ionic species (OH^-, H_3O^+, H_2O^+, e_{aq}^-) since no change in pH was observed in the course of the operation, (4) the long chain approximation [27] is used to evaluate the radical and ion reactions since the propagation reaction rates are

Table 1
Hydroxyl radical reaction with various organic compounds

Phenol + $OH^{\cdot} \xrightarrow{k_{20}}$ hydroquinone
Phenol + $OH^{\cdot} \xrightarrow{k_{21}}$ catechol
Phenol + $OH^{\cdot} \xrightarrow{k_{22}}$ resorcinol
Hydroquinone + $OH^{\cdot} \xrightarrow{k_{23}}$ pyrogallol
Hydroquinone + $OH^{\cdot} \xrightarrow{k_{24}}$ 1,2,4-benzenetriol
Hydroquinone + $OH^{\cdot} \xrightarrow{k_{25}}$ 1,4-benzoquinone
Catechol + $OH^{\cdot} \xrightarrow{k_{26}}$ pyrogallol
Catechol + $OH^{\cdot} \xrightarrow{k_{27}}$ 1,2,4-benzenetriol
Catechol + $OH^{\cdot} \xrightarrow{k_{28}}$ 1,4-benzoquinone
Resorcinol + $OH^{\cdot} \xrightarrow{k_{29}}$ pyrogallol
Resorcinol + $OH^{\cdot} \xrightarrow{k_{30}}$ 1,2,4-benzenetriol
Resorcinol + $OH^{\cdot} \xrightarrow{k_{31}}$ 1,4-benzoquinone
1,4-Benzoquinone + $OH^{\cdot} \xrightarrow{k_{32}}$ hydrobenzoquinone
Pyrogallol + $OH^{\cdot} \xrightarrow{k_{33}}$ products
1,2,4-Benzenetriol + $OH^{\cdot} \xrightarrow{k_{34}}$ products
Hydrobenzoquinone + $OH^{\cdot} \xrightarrow{k_{35}}$ products

much larger than the termination reaction rates (reactions (12)–(19)), and (5) that the initiation rates are constant over the period of the process and are functions of voltage input.

A molar species material balance was taken for each species involved in the process. Table 2 gives the material balances for molecular species and Table 3 gives the material balances for the radicals and ions used in the present model. The rate constants for reactions (4)–(19) and for the degradation reactions given in Table 1 are taken from the literature and are given in Table 4.

It has been reported that the differential equations from the material balances of the radical species show characteristics of being stiff when they are solved numerically. This is due to the fact that the time constants associated with the dynamics of the

Table 2
Molar species material balances for molecular species

$$\frac{d[PH]}{dt} = -k_{1'}\cdot[PH]\cdot[OH^-]$$

$$\frac{d[HQ]}{dt} = k_{20}\cdot[PH]\cdot[OH^-] - k_{2'}\cdot[HQ]\cdot[OH^-]$$

$$\frac{d[CC]}{dt} = k_{21}\cdot[PH]\cdot[OH^-] - k_{3'}\cdot[CC]\cdot[OH^-]$$

$$\frac{d[RS]}{dt} = k_{22}\cdot[PH]\cdot[OH^-] - k_{4'}\cdot[RS]\cdot[OH^-]$$

$$\frac{d[PG]}{dt} = k_{23}\cdot[HQ]\cdot[OH^-] + k_{26}\cdot[CC]\cdot[OH^-] + k_{29}\cdot[RS]\cdot[HO^-] - k_{32}\cdot[PG]\cdot[HO^-]$$

$$\frac{d[HHQ]}{dt} = k_{24}\cdot[HQ]\cdot[OH^-] + k_{27}\cdot[CC]\cdot[OH^-] + k_{30}\cdot[RS]\cdot[OH^-] - k_{33}\cdot[HHQ]\cdot[OH^-]$$

$$\frac{d[BQ]}{dt} = k_{25}\cdot[HQ]\cdot[OH^-] + k_{28}\cdot[CC]\cdot[OH^-] + k_{31}\cdot[RS]\cdot[OH^-] - k_{34}\cdot[BQ]\cdot[OH^-]$$

$$\frac{d[HBQ]}{dt} = k_{34}\cdot[BQ]\cdot[OH^-] - k_{35}\cdot[HBQ]\cdot[OH^-]$$

$$\frac{d[H_2O_2]}{dt} = k_{H_2O_2} + K_{13}\cdot[OH^-]^2 + k_{14}\cdot[HO_2]^2 + k_{15}\cdot[H^-]\cdot[HO_2^-]$$
$$- k_5\cdot[H^-]\cdot[H_2O_2] - k_6[OH^-]\cdot[H_2O_2] - k_{10}\cdot[e_{aq}^-]\cdot[H_2O_2]$$

$$\frac{d[H_2]}{dt} = k_9\cdot[H_2O]\cdot[e_{aq}^-][H^-] + k_{16}\cdot[H^-]^2$$

$$\frac{d[O_2]}{dt} = k_{14}\cdot[HO_2^-]^2 + k_{17}\cdot[HO_2^-]\cdot[OH^-]$$

radical species are quite different from those related to the dynamics of the molecular species [23]. Therefore, by using the pseudo-steady state approximation the dynamics of the radical species can be described by a system of coupled algebraic equations. The long chain approximation simplifies these coupled algebraic equations to a system of sequentially-coupled equations. These assumptions for radical and ion species simplifies the differential equations given in Table 3 to algebraic equations given in Table 5.

3.1. Solution strategy

The proposed model consists of a set of seven ordinary differential equations and eleven algebraic equations which can be expressed in a general form as

$$\frac{dY_i}{dt} = f_i(Y_1, Y_2, Y_3, \ldots, Y_N, X_1, X_2, \ldots, X_m), \quad i = 1, 2, \ldots, M$$

and

$$X_j = g_j(Y_1, Y_2, Y_3, \ldots, Y_n, X_1, X_2, \ldots, X_{j-1}, X_{j+1}, \ldots, X_M), \quad j = 1, 2, \ldots, N,$$

Table 3
Material balances for radical and ionic species

$$\frac{d[OH^{\cdot}]}{dt} = k_{OH^{\cdot}} + k_5 \cdot [H_2O_2] \cdot [H^{\cdot}] + k_7 \cdot [H_2O] \cdot [H_2O^+] + k_{10} \cdot [H_2O_2] \cdot [e^-_{aq}] - k_{1'} \cdot [PH] \cdot [OH^{\cdot}] - k_{2'} \cdot [HQ] \cdot [OH^{\cdot}] - k_{3'} \cdot [CC] \cdot [OH^{\cdot}] - k_{4'} \cdot [RS] \cdot [OH^{\cdot}] - k_{32} \cdot [PG] \cdot [OH^{\cdot}] - k_{33} \cdot [HHQ] \cdot [OH^{\cdot}] - k_{34'} \cdot [BQ] \cdot [OH^{\cdot}] - k_{35'} \cdot [HBQ] \cdot [OH^{\cdot}] - k_8 \cdot [e^-_{aq}] \cdot [OH^{\cdot}] - k_6 \cdot [H_2O_2] \cdot [OH^{\cdot}].$$

$$\frac{d[HO_2^{\cdot}]}{dt} = k_4[H^{\cdot}] \cdot [O_2] + k_6 \cdot [H_2O_2] \cdot [OH^{\cdot}] - k_{15}[H^{\cdot}] \cdot [HO_2^{\cdot}] - k_{17}[HO_2^{\cdot}] \cdot [OH^{\cdot}]$$

$$\frac{d[H^{\cdot}]}{dt} = k_{OH^{\cdot}} + k_{1'} \cdot [PH] \cdot [OH^{\cdot}] + k_{2'} \cdot [HQ] \cdot [OH^{\cdot}] + k_{3'} \cdot [CC] \cdot [OH^{\cdot}] + k_{4'} \cdot [RS] \cdot [OH^{\cdot}] + k_{32} \cdot [PG] \cdot [OH^{\cdot}] + k_{33} \cdot [HHQ] \cdot [OH^{\cdot}] + k_{34'} \cdot [BQ] \cdot [OH^{\cdot}] + k_{35'} \cdot [HBQ] \cdot [OH^{\cdot}] + k_4 \cdot [e^-_{aq}] [H_2O_2] - k_5 \cdot [H^{\cdot}] [O_2] - k_9 \cdot [H_2O] \cdot [e^-_{aq}] [OH^{\cdot}] + k_{11} \cdot [H^{\cdot}] [HO_2^{\cdot}]$$

$$\frac{d[e^-_{aq}]}{dt} = k^-_{e_{aq}} - k_8 \cdot [e^-_{aq}] [OH^{\cdot}] - k_9 \cdot [H_2O] [e^-_{aq}] [H^{\cdot}] - k_{10} \cdot [e^-_{aq}] \cdot [H_2O_2] - k_{11} \cdot [e^-_{aq}] \cdot [H_2O]$$

$$\frac{d[H_2O^+]}{dt} = k_{e_{aq}} - k_7 \cdot [H_2O^+] \cdot [H_2O] - k_{19} \cdot [H_2O^+] \cdot [e^-_{aq}]$$

$$\frac{d[OH^-]}{dt} = k_8 \cdot [e^-_{aq}] [OH^{\cdot}] + k_9 [H_2O] [e^-_{aq}] [H^{\cdot}] + k_{10} \cdot [e^-_{aq}] [H_2O_2] + k_{11} \cdot [H_2O] [e^-_{aq}] - k_{18} \cdot [H_3O^+] \cdot [OH^-]$$

$$\frac{d[H_3O^+]}{dt} = k_7 \cdot [H_2O^+] - k_{18} \cdot [H_3O^+] \cdot [OH^-]$$

where Y_i = concentration of ith stable molecular species, and X_j = concentration of jth radical or ionic species. In accounting for reactions (1)–(19) the values of $M = 11$ and $N = 7$ were used. This system was solved by using the Runge–Kutta–Gills Method [28]. The proposed model for phenol degradation was used to determine the initiation rate constant for the formation of aqueous electrons by fitting the experimental data for phenol degradation. Initiation rate constants for hydroxyl radicals and hydrogen peroxide were determined experimentally. Using this information, the above reactor model was used to predict the degradation of hydroquinone and the formation of hydrogen peroxide. The prediction of the model was compared with the experimental results. The experimental methods and results are discussed in subsequent sections.

4. Experimental materials and methods

Fig. 1 shows a schematic diagram of the reactor vessel used in the present investigation. A cylindrical plexiglass tube having dimensions of 5 cm inside diameter

Table 4

Rate constant (l/mol/s)	Reference
$k_4 = 1.0 \times 10^{10}$	[23]
$k_5 = 1.0 \times 10^{10}$	[23]
$k_6 = 2.7 \times 10^{7}$	[21]
$k_7 = 5.0 \times 10^{7}$	[23]
$k_8 = 3.0 \times 10^{10}$	[23]
$k_9 = 2.5 \times 10^{10}$	[23]
$k_{10} = 1.2 \times 10^{7}$	[23]
$k_{11} = 1.0 \times 10^{10}$	[23]
$k_{12} = 2.4 \times 10^{10}$	[23]
$k_{13} = 4.0 \times 10^{9}$	[23]
$k_{14} = 2.0 \times 10^{6}$	[23]
$k_{15} = 1.0 \times 10^{10}$	[23]
$k_{16} = 1.0 \times 10^{10}$	[23]
$k_{17} = 1.0 \times 10^{10}$	[23]
$k_{18} = 3.0 \times 10^{10}$	[23]
$k_{19} = 1.0 \times 10^{10}$	[23]
$k_1' = (k_{20} + k_{21} + k_{22}) = 1.85 \times 10^{10}$	[40]
$k_2' = (k_{23} + k_{24} + k_{25}) = 1.20 \times 10^{11}$	[41]
$k_3' = (k_{26} + k_{27} + k_{28}) = 1.0 \times 10^{10}$	[4]
$k_4' = (k_{29} + k_{30} + k_{31}) = 1.0 \times 10^{10}$	[4]
$k_{32} = 1.0 \times 10^{10}$	[4]
$k_{33} = 1.0 \times 10^{10}$	[4]
$k_{34} = 1.0 \times 10^{10}$	[4]
$k_{35} = 1.0 \times 10^{10}$	[4]

and 21 cm high was capped on the top and the bottom to form a watertight enclosure. During experiments, the reactor vessel typically contained 550 ml of solution and was submerged in an outer chamber containing an ice bath in order to maintain isothermal conditions (25–30 °C). Pulsed streamer corona treatment of the test solution was provided by a non-uniform point-to-plane electrode geometry. A stainless steel hollow hypodermic needle point electrode was located along the central axis of the cylindrical reactor approximately 5 cm above the bottom of the vessel. A stainless steel rounded plate ground electrode was placed at the top of the reactor opposite the high voltage discharge electrode. Although the separation distance can be varied, all experiments reported here were performed at a point-to-plane distance of 5 cm. A magnetic stirrer at the bottom of the reactor provided mixing of the solution in the reactor.

It should be noted that the active volume for the reactions induced by the corona discharge consists of a conical or hemispherical region between the point electrode and the flat ground plate electrode, and that this region is approximately $\frac{1}{3}$ of the total reactor volume. This characteristic may lead to a lower bound of the value of the rate constants involved in the actual kinetics (i.e., a conservative estimate of such a rate constant) arising from the corona discharge. The well-mixed reactor design (i.e., batch

Table 5
Pseudo-steady state approximation for radical and ionic species

$$[OH^{\cdot}] = \frac{k_{OH^{\cdot}} + (k_5 \cdot [H^{\cdot}] + k_{10} \cdot [e^-_{aq}]) \cdot [H_2O_2] + k_7 \cdot [H_2O] \cdot [H_2O^+]}{W + k_8 \cdot [e^-_{aq}] + k_6 \cdot [H_2O_2]}$$

$$[HO_2^{\cdot}] = \frac{k_4 \cdot [H^{\cdot}] \cdot [O_2] + k_6 \cdot [H_2O_2] \cdot [OH^{\cdot}]}{k_{15} \cdot [H^{\cdot}] + k_{17} \cdot [OH^{\cdot}]}$$

$$[H^{\cdot}] = \frac{k_{OH^{\cdot}} + W \cdot [OH^{\cdot}] + k_4 \cdot [e^-_{aq}][H_2O_2]}{k_{11} \cdot [HO_2^{\cdot}]}$$

$$[e^-_{aq}] = \frac{k_{e^-_{aq}}}{k_8 \cdot [OH^{\cdot}] + k_9 \cdot [H_2O][H^{\cdot}] + k_{10} \cdot [H_2O_2] + k_{11} \cdot [H_2O]}$$

$$[H_2O^+] = \frac{k_{e^-_{aq}}}{k_7 \cdot [H_2O] + k_{19} \cdot [e^-_{aq}]}$$

$$[OH^-] = k_8 \cdot [e^-_{aq}][OH^{\cdot}] + k_9 \cdot [H_2O][e^-_{aq}][H^{\cdot}] + k_{10} \cdot [e^-_{aq}][H_2O_2] + k_{11} \cdot [H_2O][e^-_{aq}]$$

$$[H_3O^+] = \frac{k_7 \cdot [H_2O^+] \cdot [H_2O]}{k_{18} \cdot [OH^-]}$$

where

$$W = k_{1'} \cdot [PH] + k_{2'} \cdot [HQ] + k_{3'} \cdot [CC] + k_{4'} \cdot [RS] + k_{32} \cdot [PG] - k_{33} \cdot [HHQ] - k_{34} \cdot [BQ] - k_{35} \cdot [HBQ]$$

reactor model) coupled with a point-to-plane electrode geometry shows this intrinsic characteristic. Further research to consider the effects of solution mixing and of the corona discharge inactive zone is underway and will be reported in future publications.

A Masterflex recirculation pump was connected to the reactor using two nylon fittings and $\frac{1}{8}$ in. diameter polyethylene tubing to allow for sample withdrawal. Typically, 5 ml samples were taken from the reactor vessel at 10 min intervals during each run. Temperature, pH, and conductivity of the solution were measured before and after each experiment.

A rotating spark gap power supply [8] is used to provide pulsed energization of the high voltage discharge electrode. Peak voltage (V_p) used was in the range of 25–40 kV, pulse width was in the range of 500–1000 ns. The repetition frequency was 60 Hz. Streamer corona propagate outward from the tip of the needle point, producing a conical discharge region. The fast-rising, short duration discharge having an average electric field of between 5 and 8 kV/cm could be sustained without sparkover. This results in the formation of more intense and uniform streamers. Positive polarity streamers are longer and cover a larger volume compared to negative polarity streamers.

Reagent grade phenol (99.7%), purified grade hydroquinone, and certified grade catechol were obtained from Fisher Scientific Inc. Analytical reagent grade sodium carbonate was obtained from Mallinckrodt, Inc. Reagent grade acetonitrile (assay

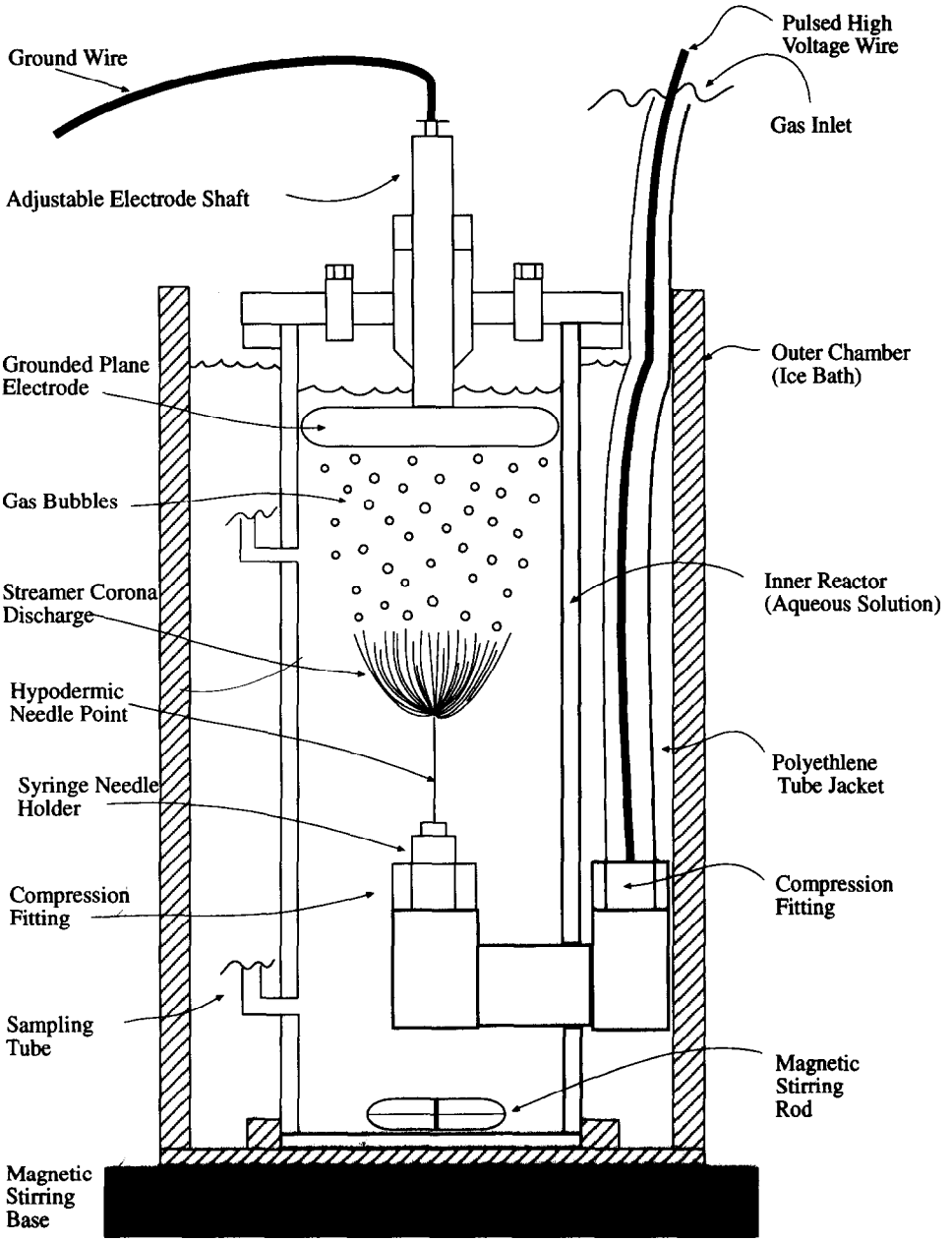

Fig. 1. Schematic of pulsed streamer corona reactor.

98.73%) was obtained from Mallinckrodt, Inc. Glacial acetic acid (99.71% w/w) and reagent grade potassium hydrogen phthalate were obtained from Fisher Scientific, Inc. Ammonium molybdate (4.8% w/v) was obtained from Lab-Chem, Inc. Certified grade sulfuric acid (1 *N*) was obtained from Fisher Scientific, Inc. Ultra-pure carrier grade helium and AA grade nitrous oxide were obtained from Air Products and Chemicals, Inc.

A Perkin-Elmer HPLC unit with a reversed phase C-18 column obtained from Supelco, Inc., was used to measure the concentration of phenol and other organic compounds. The UV detector wavelength was set at 280 nm. An isocratic method was used with the chromatography pump conditions set to 1.5 ml/min. The mobile phase was prepared by dissolving 0.5% acetic acid and 5.0% acetonitrile in deionized water [11, 24, 25]. Sample analysis was performed immediately after removal from the reactor. Peak heights were used to determine both the phenol concentration and hydroquinone concentration after calibration with standard solutions.

A Beckman UV–Vis spectrophotometer was used to measure the concentration of hydrogen peroxide by a colorimetric method developed by Ghormley [18, 19]. Iodide ion is oxidized by hydrogen peroxide in neutral or slightly acidic solution, and the absorption of I_3^- is measured at 350 nm. The iodide reagent was prepared immediately before the experiment by mixing equal volumes of two solutions containing: (a) 10 ml of 1% ammonium molybdate, 1 g of sodium hydroxide, and 33 g of potassium iodide, and (b) 10 g of potassium hydrogen phthalate, each diluted to 500 ml by deionized water. The alkaline iodide solution is stable but in the mixed reagent the iodide is slowly oxidized by dissolved oxygen. A measured volume of sample (1 ml) was diluted to definite volume (10 ml) with deionized water and reagent, with reagent making up one-half of the final volume (5 ml). The optical density of the sample was measured at 350 nm after calibrating with deionized water. The concentration of hydrogen peroxide is given by $C = 40dD$, where C = concentration in units of 10^{-6} M, d = dilution factor = 10, and D = optical density.

Phenol solutions were prepared by dissolving 2.8–3.0 ml of 5 m*M* stock phenol solution in 550 ml of deionized water. The final concentration was 2.5–2.9 mg/l. The solution was then transferred into the pulsed streamer corona discharge reactor. The temperature was kept constant at 25–30 °C. The applied peak pulsed voltage was controlled at 25, 30, 35, or 40 kV. For the experiments conducted in the presence of sodium carbonate, the phenol solutions were prepared in sodium carbonate solution. The alkalinity of the sodium carbonate solutions used was in the range of 100–500 ppm as $CaCO_3$.

Hydroquinone solutions were prepared in deionized water. The concentration of hydroquinone solutions used was in the range of 2.7–10 mg/l. Hydrogen peroxide formation was determined under two different conditions: (1) deionized water at neutral pH with the solution saturated with oxygen, (2) deionized water with sodium carbonate (100 ppm as calcium carbonate) at pH 3–3.5 (pH was adjusted by using 1 *N* sulfuric acid) with the solution saturated with helium.

Temperature, conductivity and pH of the solutions were measured before and after each experiment. No pH or temperature variation was observed during the course of

these experiments. During each hour-long experiment, the current across the reactor electrodes was recorded at intervals of 10 min.

5. Results and discussion

A series of experiments was performed to study the chemical reaction mechanisms occurring in the pulsed streamer corona discharge process in the aqueous phase. Specifically, various experimental conditions were utilized to determine the initiation rates for the formation of hydroxyl radicals, hydrogen peroxide, and aqueous electrons. This is discussed and analyzed as follows.

5.1. Determination of initiation rate for the formation of hydroxyl radicals

The rate of formation of hydroxyl radicals was determined using a pseudo-steady state approach which has previously been successfully used to study the thermal production of $OH^{\cdot}$ radicals in ozone-treated natural water samples [4], the photoproduction of $OH^{\cdot}$ in neutral water samples [29,30], and $OH^{\cdot}$ production from nitrate ions [31].

The rate of generation of $OH^{\cdot}$ from the corona by reaction (1) is $k_{OH^{\cdot}}$, and therefore the rate of $[OH^{\cdot}]$ reaction including scavenging by scavengers S is

$$r_S = (k_S[S] + k_P[P])[OH^{\cdot}]. \tag{20}$$

If P, the probe compound, is very dilute in comparison to the scavenger S, then $k_S[S] \gg k_P[P]$ and $r_S = k_S[S][OH^{\cdot}]$.

The molar species balance for hydroxyl radicals can be written as

$$\frac{d[OH^{\cdot}]}{dt} = k_{OH^{\cdot}} - r_S. \tag{21}$$

Assuming pseudo-steady state for hydroxyl radicals,

$$\frac{d[OH^{\cdot}]}{dt} = 0 \tag{22}$$

i.e., the scavenging rate of $OH^{\cdot}$ becomes equal to the formation rate of $OH^{\cdot}$,

$$k_{OH^{\cdot}} = r_S$$

and $[OH^{\cdot}]_{ss}$, the hydroxyl radical concentration, becomes

$$[OH^{\cdot}]_{ss} = k_{OH^{\cdot}}/(k_S[S]). \tag{23}$$

The oxidation rate ($M\,s^{-1}$) of the probe compound (phenol in this case) is given by

$$-d[P]/dt = k_P[OH^{\cdot}]_{ss}[P] = k_{expt}[P]. \tag{24}$$

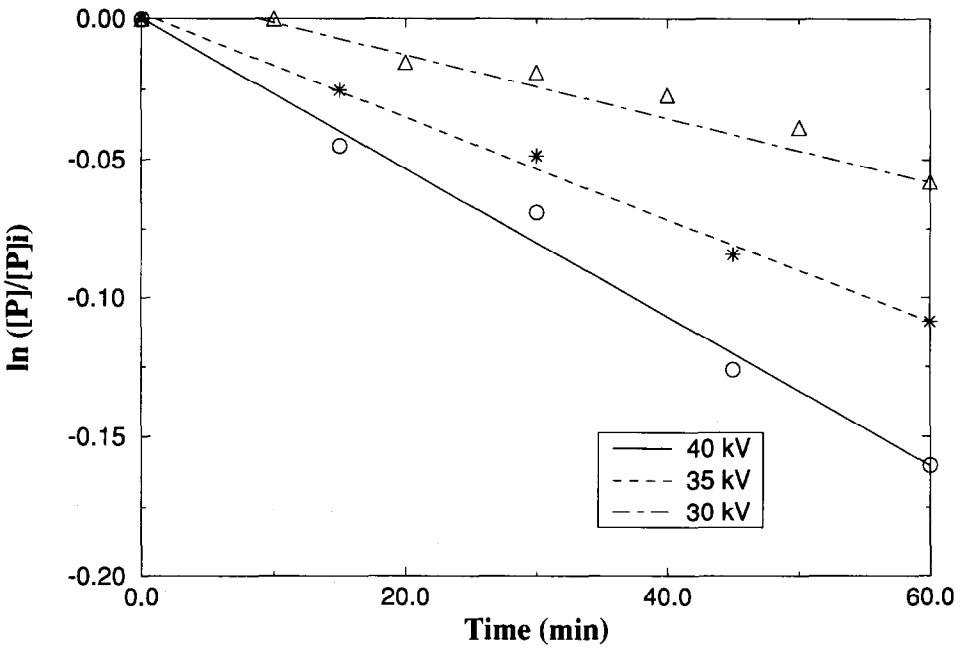

Fig. 2. Determination of rate of formation of OH·.

Under conditions in which the fractional change in the scavenger concentration is insignificant compared to that of the probe compound, the overall reaction is pseudo first-order overall, with a first-order rate constant, k_{expt}. The k_{expt} is determined by measuring the degradation of phenol in the presence of 200 ppm CO_3 ions as shown in Fig. 2.

Since the second-order rate constant, k_P, and the scavenging rate constant, k_S, are known from the literature [3], $k_{OH\cdot}$ can be calculated by combining Eqs. (23) and (24) to give

$$k_{OH\cdot} = \frac{k_{expt}(k_S[S])}{k_P}. \tag{25}$$

The initial carbonate concentration was 200 ppm as calcium carbonate, and $k_{OH\cdot}$ was determined for three different average power inputs. Since the corona onset occurs at the applied pulsed voltage of 19 kV as shown in Fig. 3 [32], and sparkover takes place above an applied pulsed voltage of 42 kV, the applied pulsed voltage was varied in this particular range. It was observed that the current across the reactor electrode was approximately constant during the period of the process for a constant applied pulsed voltage. The average power input to the reactor was in the range of 40–150 watts. Table 6 shows the values of $k_{OH\cdot}$ with a 95% confidence limit (for three repeats at each point) for different average power and voltage inputs. It is clear that

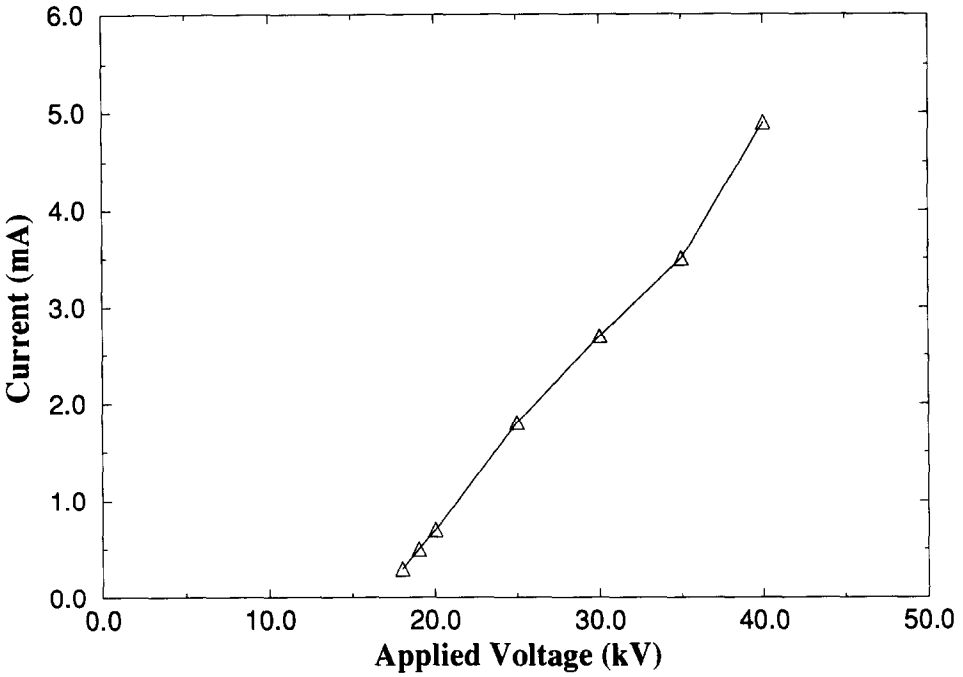

Fig. 3. Variation of current ($t = 0$) across reactor with applied pulsed voltage.

Table 6
Rate of formation of OH·

Applied voltage (kV)	Average power input per 550 ml (watts)	$k_{OH\cdot}$ ($M\,s^{-1}$)
30	45	$4.1 \times 10^{-10} \pm 3.3 \times 10^{-11}$
35	85	$6.16 \times 10^{-10} \pm 4.75 \times 10^{-11}$
40	128	$10.19 \times 10^{-10} \pm 6.26 \times 10^{-11}$

the rate of production of hydroxyl radicals increases with increases in the voltage and power input.

5.2. *Determination of initiation rate for the formation of hydrogen peroxide*

The production of hydrogen peroxide by pulsed streamer corona discharge in deionized water at neutral pH has been studied earlier [12]. The formation of hydrogen peroxide due to pulsed streamer corona discharge in deionized water takes place through reactions (2), (13)–(15) which makes it difficult to determine $k_{H_2O_2}$. In the

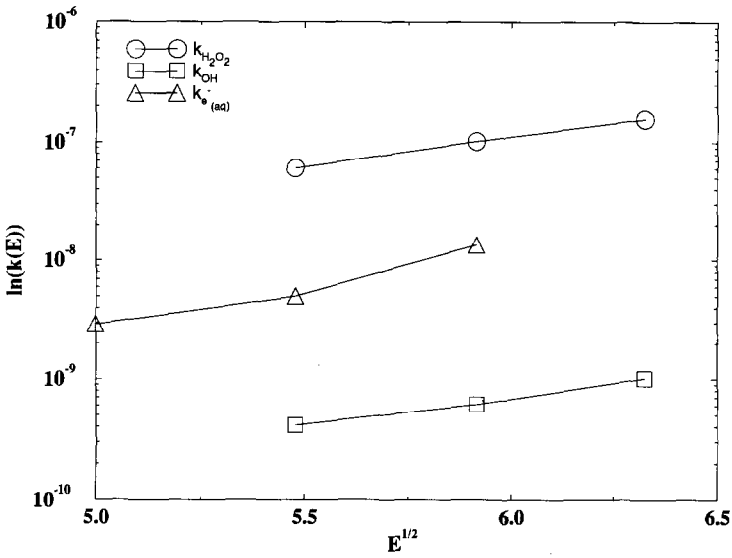

Fig. 4. Variation of $k(E)$ with electric field for three reaction rate constants.

presence of carbonate ions

$$Na_2CO_3 \rightleftharpoons 2Na^+ + CO_3^{2-}, \tag{26}$$

$$CO_3^{2-} + OH^{\cdot} \xrightarrow{k_5} CO_3^{-\cdot} + OH^-, \tag{27}$$

$$CO_3^{-\cdot} + H^{\cdot} \longrightarrow CO_3^{2-} + H^+. \tag{28}$$

Thus, in the absence of oxygen, reactions (27) and (28) dominate over reactions (5), (6), (13)–(15). The rate of formation of hydrogen peroxide is therefore given by

$$\frac{d[H_2O_2]}{dt} = k_{H_2O_2}. \tag{29}$$

In the present study, all experiments to determine formation of hydrogen peroxide were performed at pH = 3.0–3.5 with carbonate concentration of 100 ppm as calcium carbonate since hydrogen peroxide is more stable at low pH (3.0–3.5) [18]. Figs. 5(a)–(c) show the production of hydrogen peroxide for three different applied pulsed voltages under these conditions. These figures show an approximately linear increase in hydrogen peroxide concentration with respect to time, as is expected from Eq. (29).

For each voltage, $k_{H_2O_2}$ is determined from the slope of the plot. It was observed that the current across the reactor electrode was approximately constant at constant applied pulsed voltage during the period of the process. Table 7 shows the values of

Table 7
Rate of formation of H_2O_2

Applied voltage (kV)	Average power input per 550 ml (W)	$k_{H_2O_2}$ ($M\,s^{-1}$)
30	75	$6.06\times10^{-8}\pm3.1\times10^{-9}$
35	105	$10.22\times10^{-8}\pm5.24\times10^{-9}$
40	140	$15.67\times10^{-8}\pm8.28\times10^{-9}$

$k_{H_2O_2}$ with a 95% confidence limit based on three repeats for each different average power input. The results show that the production of hydrogen peroxide increases with an increase in the electric field within the range studied.

The effect of electric field on reaction rate constants has been considered by Kuskova [33], where it was found that using the theory of ion dissociation,

$$k(E) = k(0)\exp[2\sqrt{Ee^3/\varepsilon}/k_BT],$$

where E is the electric field, e is the electron charge, ε is the electrical permitivity of the solution, k_B is Boltzman's constant, and T is the absolute temperature. Fig. 4 shows a plot of $\ln k(E)$ vs. $\sqrt{E}$ for the three reaction rate constants determined in this study. This relationship appears to hold over the range of conditions studied and thus gives some indication that electrical field induced ion dissociation is important in the pulsed streamer corona process. It should be noted that this expression does not explicitly include the effects of current.

5.3. Determination of initiation rate for the formation of aqueous electrons

In the radiolysis of water, the production of hydroxyl radicals can be enhanced by using oxidizing conditions [21]. The most convenient way of obtaining almost totally oxidizing conditions is to keep the solution saturated with nitrous oxide (N_2O), which reacts with aqueous electrons to produce hydroxyl radicals by

$$e^-_{aq} + N_2O \rightarrow N_2 + O^- \xrightarrow{H_2O} OH^{\cdot} + OH^-. \tag{30}$$

It was observed in the present study that there was little effect on the degradation of phenol by keeping the reactor solution under oxidizing conditions [32]. This indicates that the rate of formation of hydroxyl radicals due to pulsed streamer corona is much greater than that from the reaction of aqueous electrons and N_2O. The molar species material balance for the hydroxyl radical is

$$d[OH^{\cdot}]/dt = k_{OH^{\cdot}} + k'[N_2O][e^-_{aq}] - k_P[P][OH^{\cdot}]. \tag{31}$$

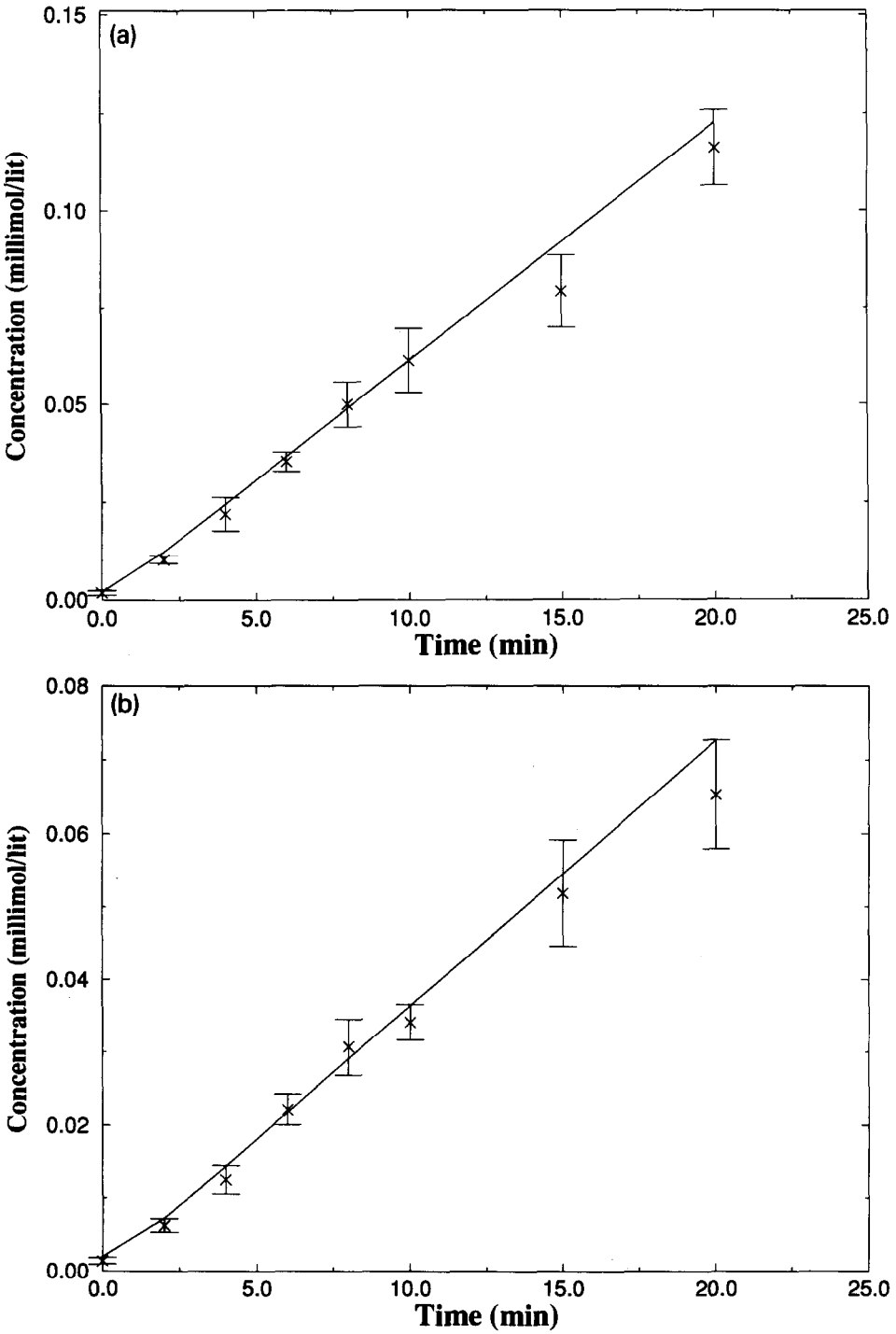

Fig. 5. (a) Formation of H_2O_2 at 100 ppm CO_3^{2-} and 30 kV. (b) Formation of H_2O_2 at 100 ppm CO_3^{2-} and 35 kV. (c) Formation of H_2O_2 at 100 ppm CO_3^{2-} and 40 kV.

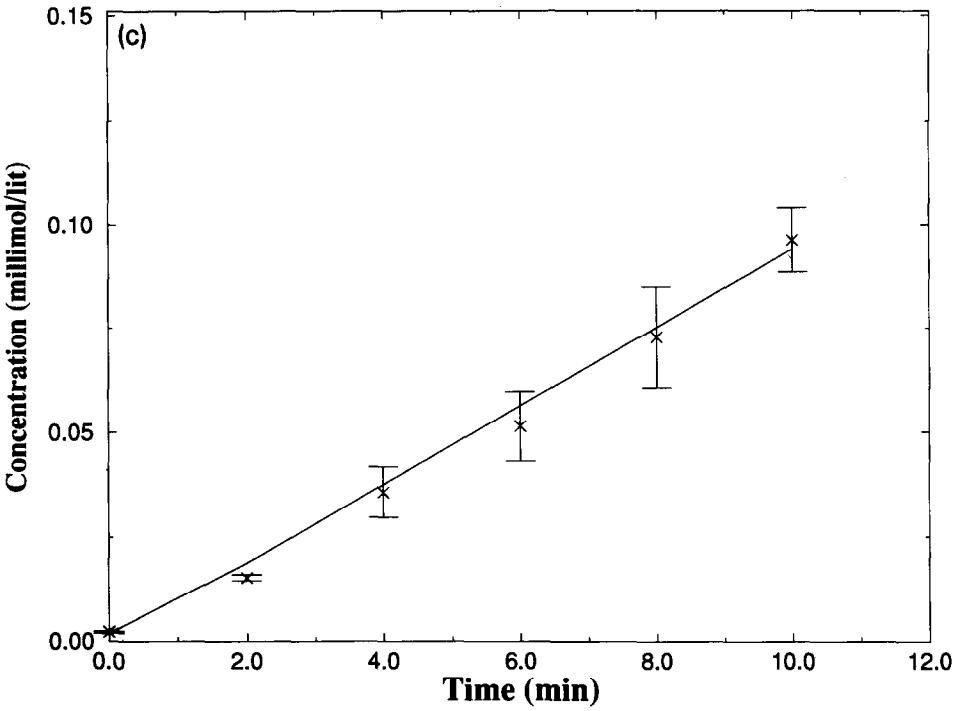

Fig. 5. Continued.

The present experiments show that $k_{OH} \gg k'[N_2O][e^-_{aq}]$ since the addition of N_2O had no effect on phenol degradation. Therefore, an indirect method was employed in order to determine the rate of formation of aqueous electrons. A model consisting of molar species material balance equations coupled with the kinetics of the chemical reactions for each species was developed as described above. The rate of formation of aqueous electrons was determined by fitting the experimental data of phenol degradation to the model. This data is shown in Fig. 6 and shows a reasonable match over the range of experimental conditions used in the present study. It was assumed here that the initiation rate constants were independent of time during the period of the process. Table 8 shows values of $k_{e^-_{aq}}$ for different average power inputs. The production of aqueous electrons increases with increases in the applied pulsed voltage.

5.4. Comparison of the pulsed streamer corona and γ-radiation processes

The rates of formation of radical and molecular species shown above were determined for different applied pulsed voltages. The large quantities of hydrogen peroxide generated by the aqueous phase discharge are consistent with modeling work performed for pulsed discharges carried out in a high humidity gas phase [34]. The

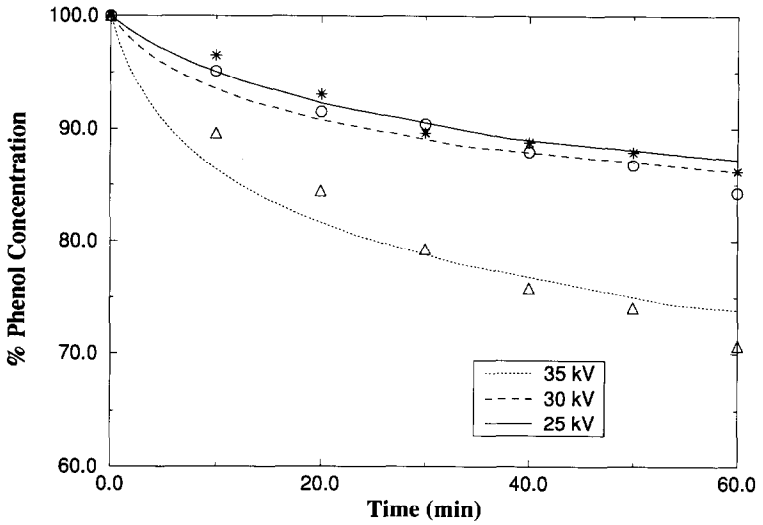

Fig. 6. Determination of $k_{e_{aq}^-}$ by experimental data fit to the model.

Table 8
Rate of formation of e_{aq}^-

Applied voltage (kV)	Average power input per 550 ml (W)	$k_{e_{aq}^-}(M\,s^{-})$
25	75	2.9×10^{-9}
30	110	5.0×10^{-9}
35	157.5	13.50×10^{-9}

relative yields of radical and molecular species from the present work and from radiation processes [7] are compared in Table 9. It is clear that the pulsed streamer corona discharge process produces a considerably larger quantity of hydrogen peroxide per molecule of hydroxyl radical and aqueous electron than the γ-radiation process. In the presence of an iron salt such as ferrous sulfate in the solution, hydrogen peroxide produces a large number of hydroxyl radicals through Fenton's reaction, as shown in previous work [8], and as given by the reaction

$$Fe^{2+} + H_2O_2 \rightarrow OH^{\cdot} + OH^{-} + Fe^{3+}. \quad (32)$$

A number of other wastewater treatment methods utilize Fenton's reaction, and comparison with these methods will be presented in future communications.

5.5. *Identification of oxidation products*

The oxidation products of phenol treated by pulsed streamer corona were identified by comparing the retention time in the C-18 HPLC column of product peaks and

Table 9
Relative yields of radical and molecular species

Radiation processes	Pulsed corona process
$\frac{G_{H_2O_2}}{G_{OH}} = 0.25–0.27$	$\frac{k_{H_2O_2}}{k_{HO}} = 100–105$
$\frac{G_{H_2O_2}}{G_{e^-_{aq}}} = 0.21–0.22$	$\frac{k_{H_2O_2}}{k_{e^-_{aq}}} = 20–21$
$\frac{G_{e^-_{aq}}}{G_{OH}} = 0.81–1.03$	$\frac{k_{e^-_{aq}}}{k_{OH}} = 45–50$

standard solution peaks. It was observed that the primary oxidation products of phenol are hydroquinone, catechol and resorcinol. These are the common oxidation products of phenol observed in most advanced oxidation processes such as ozonation [35], UV photolysis [36], supercritical water oxidation [37], UV–H_2O_2 oxidation, and wet air oxidation [38]. Since hydroquinone is a primary oxidation product of phenol, the oxidation of hydroquinone was studied.

5.6. Comparison of model and experiment

Figs. 7(a)–(c) show a comparison between the predictions of the reactor model and experimental data for the formation of hydrogen peroxide in deionized water. A comparison between the reactor model behavior and the experiments have been performed for three different voltages, i.e., at 25 kV (Fig. 7(a)), at 30 kV (Fig. 7(b)), and at 35 kV (Fig. 7(c)). The model results match the experimental data satisfactorily. At higher voltage and power input to the reactor, the model predicts approximately 10% higher concentration of hydrogen peroxide, see for example, Fig. 7(c). The possible reason for this could be the dissociation of hydrogen peroxide due to corona discharge [11] by

$$H_2O_2 \rightarrow 2OH^{\cdot}. \tag{33}$$

The hydrogen peroxide formed through reaction (2) could dissociate due to the photon flux [39] of the pulsed corona by reaction (33), resulting in the production of more hydroxyl radicals. This reaction is not included in the present model since no information is presently available on the quantity of UV photon flux involved in the pulsed corona discharge.

The model was also used to predict the degradation of hydroquinone for different initial concentrations at a voltage of 35 kV. Fig. 8 shows the predictions of the model and the experimental data for hydroquinone degradation. Initially, for the three different initial concentration levels the model predicts higher levels of hydroquinone degradation, but after about 40 min the trend is reversed and the model predicts lower

degradation of hydroquinone. A possible reason for the kind of behavior found in this comparison is the assumption that the initiation rate constants are independent of the current levels over the period of the process. As shown in Fig. 9 for the case of 35 kV applied voltage and a solution of deionized water, the current across the reactor electrodes increases with respect to time at constant applied pulsed voltage due to a change in the conductivity of the solution during the process. It should be noted that in the high conductivity solution (i.e., with added carbonate salts) the current was not observed to change significantly during the course of an experiment. The assumption of constant initiation rates over the entire course of the experiments with hydroquinone in deionized water may therefore no longer be valid. This can be taken into consideration by assuming current as a function of time at constant applied pulsed voltage. It was observed that in deionized water, the current is an approximately linear function of time at constant applied voltage through

$$I(t) = I_0 + At, \tag{34}$$

where I_0 = initial current, $A = (I(t) - I_0)/t_j$, t_j = final time, and t = time. An empirical modification of the initiation reaction rate constants to account for current can be made [32] and the resulting effects on the hydroquinone degradation calculated.

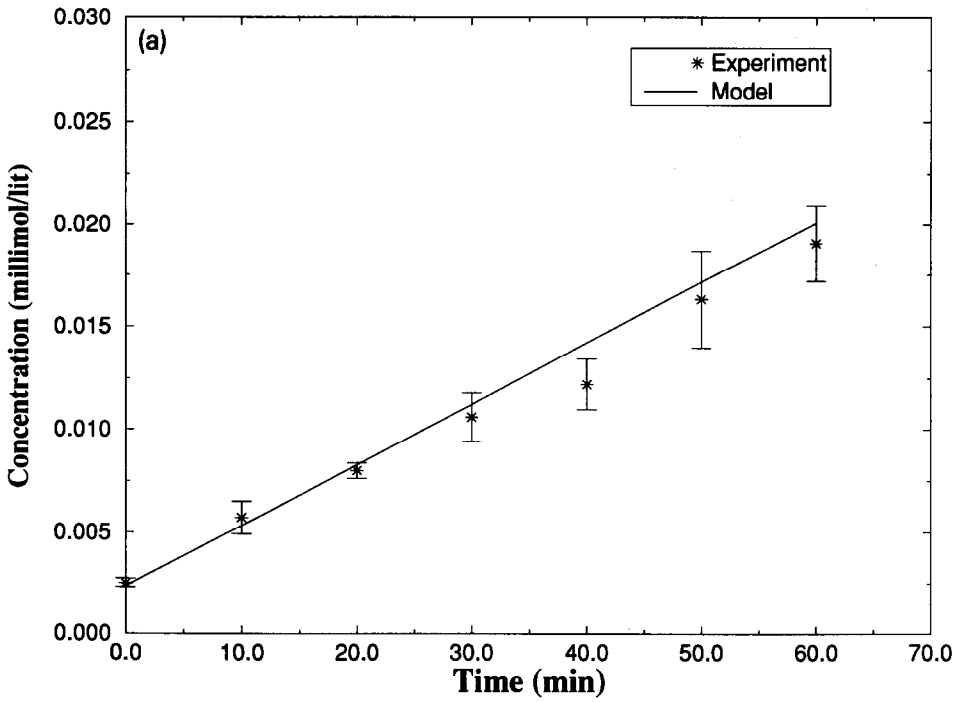

Fig. 7. (a) Formation of H_2O_2 at 25 kV: model and experiment. (b) Formation of H_2O_2 at 30 kV: model and experiment. (c) Formation of H_2O_2 at 35 kV: model and experiment.

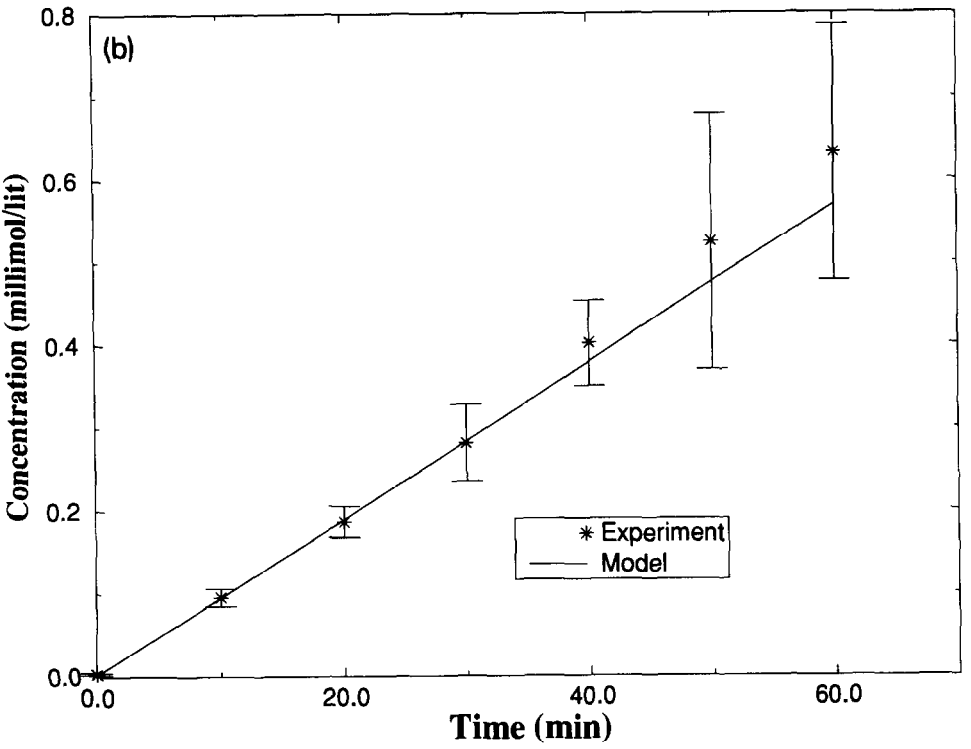

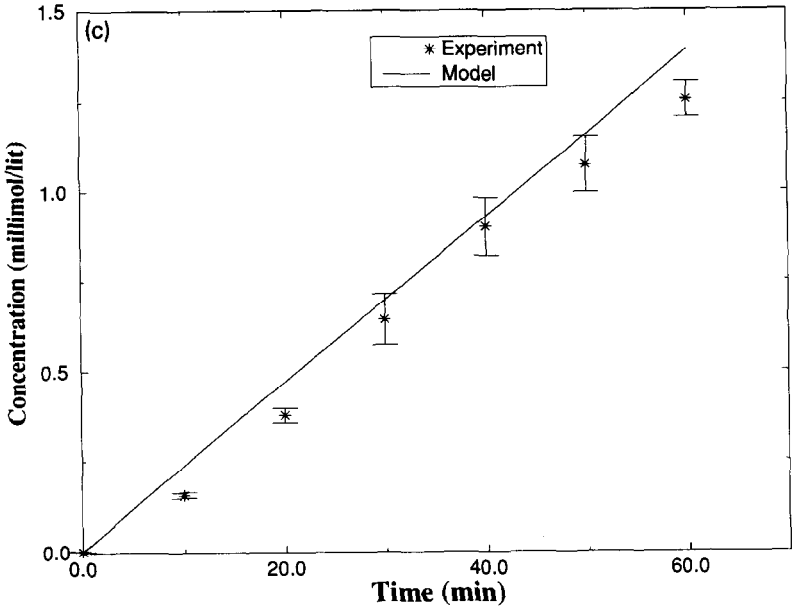

Fig. 7. Continued.

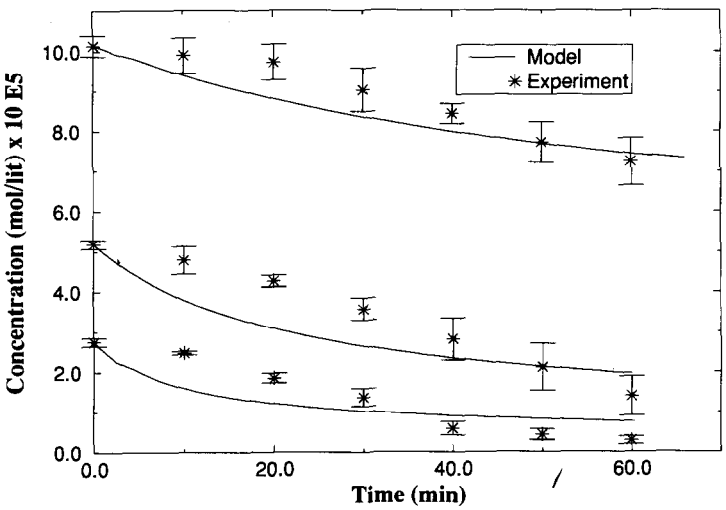

Fig. 8. Degradation of hydroquinone at 35 kV: model (using average power input) and experiment.

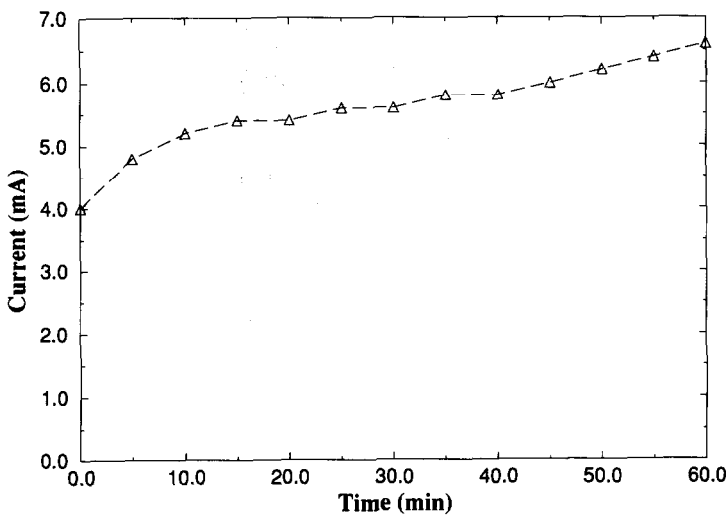

Fig. 9. Variation of current across the reactor with time at 35 kV.

The results of the adjusted reactor model and experiment are shown in Fig. 10. The model results match adequately with the experimental results for most of the duration of the experiment. Specifically, for high initial concentrations of hydroquinone, the model results match very well with the experimental results. Further work, however, must be performed to improve the model behavior at short reaction times. In this

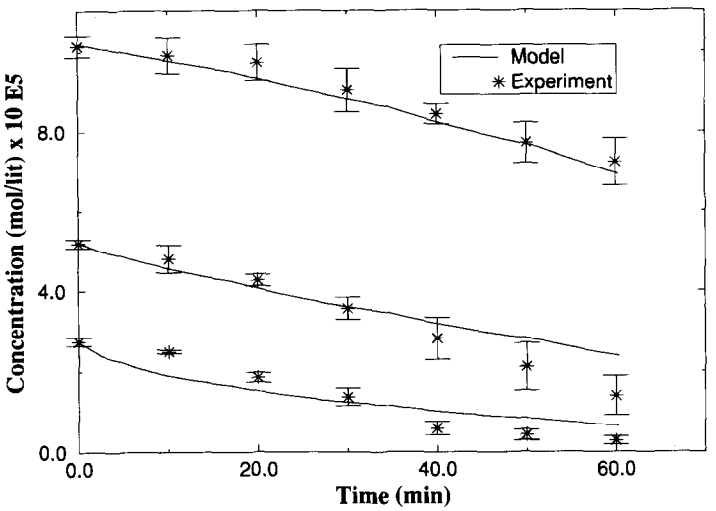

Fig. 10. Degradation of hydroquinone at 35 kV: model (using variation in power input) and experiment.

regard, the effect of removing the steady state assumptions for radicals and ions should be explored.

6. Summary and conclusions

It has been shown in the present study that pulsed streamer corona discharge treatment of aqueous solutions produces a significant quantity of hydroxyl radicals and hydrogen peroxide. The rates of formation of hydroxyl radicals and hydrogen peroxide due to the pulsed streamer corona discharge have been determined using the free radical scavenging property of carbonate ions. A reactor model for describing the behavior of the pulsed streamer corona in an aqueous phase well-mixed reactor has been developed. The rate of formation of aqueous electrons was determined by fitting the experimental data for phenol degradation to the kinetic model. Effects of the time-averaged power input on the rates of formation of radical and molecular species were also studied in the range of operation of the laboratory reactor.

It was observed in the laboratory experiments that the rates of formation of hydroxyl radicals and aqueous electrons increases in a non-linear fashion with respect to the average power input, while the rate of formation of hydrogen peroxide increases approximately linearly with respect to average power input within the experimental range. It was also observed that the relative yield of hydrogen peroxide with respect to hydroxyl radicals was much larger than that found by other workers investigating the γ-radiation process. This indicates that the pulsed streamer corona discharge process yields larger quantities of hydrogen peroxide than hydroxyl radicals. This is important from the viewpoint of utilizing Fenton's reactions, where hydrogen peroxide reacts with iron to produce more hydroxyl radicals by reaction (35).

Reiterated, the pulsed streamer corona discharge process in the aqueous phase can produce hydrogen peroxide in situ. This may represent an important advantage of the pulsed streamer corona process over other organic waste oxidation processes, such as the UV–H_2O_2 oxidation processes which use separately produced and injected hydrogen peroxide.

The reactor model proposed here was tested for the formation of hydrogen peroxide in deionized water, and the results adequately match that of the experiments. The model results for the degradation of hydroquinone showed the expected trends in comparison to the experimental results. The reactor model was improved by assuming that the rate constants for the initiation reactions are time dependent functions of the average current across the reactor electrodes. Moreover, this functionality is assumed to be linear with respect to time (due to a change in the conductivity of the solution) at constant applied pulsed voltage. The initiation rate constants, therefore, must reflect such a change over this same period. The results of the modified reactor model match satisfactorily with those of the experiment. The model follows experimental results adequately for high initial hydroquinone concentration ($>5.4\times10^{-5}$ M). Further work is required to improve the present model to predict degradation of phenolic compounds at low initial concentration ($<5.4\times10^{-5}$ M) and for short times.

The oxidation pathways for phenol and hydroquinone were assumed on the basis of literature information. It was observed that hydroquinone, catechol, and resorcinol are the primary oxidation products of phenol. In addition, three other compounds were observed during the oxidation of hydroquinone which have not yet been identified.

7. Nomenclature

$[PH]$ = concentration of phenol
$[HQ]$ = concentration of hydroquinone
$[CC]$ = concentration of catechol
$[RS]$ = concentration of resorcinol
$[PG]$ = concentration of pyrogallol
$[HBQ]$ = concentration of hydrobenzoquinone
$[HHQ]$ = concentration of 1,2,4-benzetriol
$[BQ]$ = concentration of benzoquinone
$[H_2O_2]$ = concentration of hydrogen peroxide
$[H_2]$ = concentration of hydrogen
$[O_2]$ = concentration of oxygen
$[OH^{\cdot}]$ = concentration of hydroxyl radical
$[HO_2^{\cdot}]$ = concentration of hydroperoxyl radical
$[H^{\cdot}]$ = concentration of atomic hydrogen
$[e_{aq}^-]$ = concentration of aqueous electron
$[H_2O^+]$ = concentration of H_2O^+ ion
$[H_3O^+]$ = concentration of H_3O^+ ion
$[OH^-]$ = concentration of OH^- ion

t = time
Y_i = concentration of the ith stable series
X_i = concentration of the ith radical species

Acknowledgements

We would like to thank the Department of Chemical Engineering at the FAMU/FSU College of Engineering and The Florida State University for support of this research. In addition, we acknowledge the Nuclear Services Department at The Florida State University for allowing us the use of the high voltage pulsed power supply and laboratory space. A preliminary version of this paper was presented at the Annual Meeting of the AIChE in St. Louis, Missouri, in November 1993, as paper number 160c.

References

[1] D.F. Ollis, E. Pelizzetti and N. Serpone, Destruction of water contaminants, Environ. Sci. Technol., 25(9) (1991) 1523.
[2] R. Venkatadri and R.W. Peters, Chemical oxidation technologies: ultraviolet light/hydrogen peroxide, Fenton's reagent, and titanium dioxide-assisted photocatalysis, Hazard. Waste Hazard. Mater., 10(2) (1993) 107.
[3] J. Hoigne and H. Bader, The role of hydroxyl radical reactions in ozonation processes in aqueous solutions, Water Res., 10 (1976) 377.
[4] J. Hoigne and H. Bader, Ozonation of water: selectivity and rate of oxidation of solutes, Ozone Sci. Eng., 1 (1979) 357.
[5] A.P. Davis and C.P. Huang, The removal of substituted phenols by a photocatalytic oxidation process with cadmium sulfide, Water Res., 24(5) (1990) 543.
[6] M.G. Nickelsen, W.J. Cooper, C.N. Kurucz and T.D. Waite, Removal of benzene and selected alkyl-substituted benzenes from aqueous solution utilizing continuous high-energy electron irradiation, Environ. Sci. Technol., 26 (1992) 144.
[7] E.H. Bryan, Radiation energy treatment of water wastewater and sludge, Am. Soc. Civil Engineers, New York, 1992.
[8] A.K. Sharma, B.R. Locke, P. Arce and W.C. Finney, A preliminary study of pulsed streamer corona discharge for the degradation of phenol in aqueous solutions, Hazard. Waste Hazard. Mater., 10(2) (1993) 209.
[9] K. Warner, A. Sharma, B.R. Locke, P. Arce, W.C. Finney and A. Joshi, Application of pulsed streamer corona discharges for treatment of petroleum contaminated groundwater, ACS Florida Sections Meeting, Orlando, FL, 1993.
[10] J.S. Clements, M. Sato and R.H. Davis, Preliminary investigation of prebreakdown phenomena and chemical reactions using a pulsed high voltage discharge in water, IEEE Trans. Ind. Appl., IA-23 (1987) 1372.
[11] A.K. Sharma, High voltage pulsed streamer corona discharges for the removal of organic contaminants from aqueous solutions, Masters Thesis, FAMU/FSU College of Engineering, Tallahassee, FL, 1993.
[12] J. Huff, Production of hydrogen peroxide in the pulsed streamer corona process, Undergraduate Honors Thesis, FAMU/FSU College of Engineering, Tallahassee, FL, 1993.
[13] A.J. Swallow, Radiation Chemistry of Organic Compounds, Pergamon Press, Oxford, 1960.
[14] M. Sudoh, T. Kodera, K. Sakai, J.Q. Zhang and K. Koide, Oxidation degradation of aqueous phenol effluent with electrogenerated Fenton's reagent, J. Chem. Eng. Japan, 19 (1986) 513–518.

[15] G. Hughes, Radiation Chemistry, Clarendon Press, Oxford, 1973.
[16] J. Bednar, Theoretical Foundations of Radiation Chemistry, Kluwer Academic Publishers, Dordrecht, 1969.
[17] J.W.T. Spinks and R.J. Woods, An Introduction to Radiation Chemistry, Wiley, New York, 1976.
[18] C.J. Hochanadel, Effects of cobalt γ-radiation on water and aqueous solutions, J. Phys. Chem., 56 (1952) 587.
[19] E.J. Hart, The radical pair yield of ionizing radiation in aqueous solutions of formic acid, J. Phys. Chem., 56 (1952) 594.
[20] M. Burton and K. Funabashi, Chemical Reactions in Electrical Discharges, in: R.F. Gould (Ed.), Adv. in Chem. Ser., 80 (1969) 140.
[21] G. Buxton, Radiation chemistry of the liquid state: (1) water and homogeneous aqueous solutions, in: Farhatziz and M.A.J. Rodgers (Eds.), Radiation Chemistry: Principles and Applications, VCH Publishers, New York, 1987, pp. 321–348.
[22] A. Chatterjee, Interaction of ionizing radiation with matter, in: Farhatziz and M.A.J. Rodgers (Eds.), Radiation Chemistry: Principles and Applications, VCH Publishers, New York, 1987, pp. 1–128.
[23] J.L. Magee and A. Chatterjee, Theoretical aspects of radiation chemistry, in: Farhatziz and M.A.J. Rodgers (Eds.), Radiation Chemistry: Principles and Applications, VCH Publishers, New York, 1987, pp. 137–139.
[24] M.D. Gurol and P.C. Singer, Dynamics of ozonation of phenol-I, Water Res., 17 (1983) 1163.
[25] M.D. Gurol and P.C. Singer, Dynamics of ozonation of phenol-II, Water Res., 17 (1983) 1170.
[26] K. Okamoto, Y. Yamamoto, H. Tanaka, M. Tanaka and A. Itaya. Heterogeneous photocatalytic decomposition of phenol over TiO_2 powder, Bull. Chem. Soc. Jpn., 58 (1985) 2015.
[27] G.R. Gavalas, The long chain approximation in free radical reaction systems, Chem. Eng. Sci., 21 (1966) 133.
[28] F.M. White, Viscous Fluid Flow, McGraw-Hill, New York, 1974.
[29] W.R. Haag and C.C.D. Yao, Rate constants for reaction of hydroxyl radicals with several drinking water contaminants, Environ. Sci. Technol., 26 (1992) 1005.
[30] R.G. Zepp, B.C. Faust and J. Hoigne. Hydroxyl radical formation in aqueous reaction (pH 3–8) of iron (II) with hydrogen peroxide: the photo-Fenton reaction, Environ. Sci. Technol., 26 (1992) 313.
[31] R.G. Zepp, J. Hogine and H. Bader, Nitrate-induced photooxidation of trace organic chemicals in water, Environ. Sci. Technol., 21(5) (1987) 443–450.
[32] A.A. Joshi, Formation of hydroxyl radicals, hydrogen peroxide, and aqueous electrons by pulsed streamer corona discharge in aqueous solutions, MS Thesis, FAMU/FSU College of Engineering, Tallahassee, FL, 1994.
[33] N.I. Kuskova, Mechanism of leader propagation in water, Soc. Phys. Tech. Phys., 28(5) (1993) 591–592.
[34] R. Peyrous, P. Pignolet and B. Held, Kinetic simulation of gaseous species created by an electrical discharge in dry or humid oxygen, J. Phys. D. Appl. Phys., 22 (1989) 1658.
[35] M.D. Gurol and R. Vatistas, Oxidation of phenolic compounds by ozone and ozone + UV radiation: a comparative study, Water Res., 21 (1987) 895–900.
[36] J. Peral, J. Casado and J. Domenech, Light-induced oxidation of phenol over ZnO powder, J. Photochem. Photobiol. A: Chem., 44 (1988) 209.
[37] T.D. Thornton and P.E. Savage, Phenol oxidation in supercritical water, J. Supercritical Fluids, 3 (1990) 240.
[38] H.S. Joglekar, S.D. Samant and J.B. Joshi, Kinetics of wet air oxidation of phenol and substituted phenols, Water Res., 25(2) (1991) 135.
[39] S. Lunak and P. Sedlak, Photoinitiated reactions of hydrogen peroxide in liquid phase, J. Photchem. Photobiol. A: Chem., 68 (1992) 1.
[40] D. Grosjean, Atmospheric chemistry of toxic contaminants, 1. Reaction rates and atmospheric persistence, J. Air. Waste Manag. Assoc., 40 (1990) 1397.
[41] J.K. Kochi, Free Radicals, Wiley, New York, 1993.